Electronic Supplementary Information

Fe^{3+} induced etching and hydrolysis precipitation strategy triggers Fe-Co hydroxide nanotube array toward hybrid water electrolysis

Chengyi Lu,[a,b,c] Xiao Shi,[d] Juchen Li,[a,b] Xuefei Wang,[a,b,c] Silun Luo,[a,b] Wenxin Zhu*[d] and Jianlong Wang*[d]

[a] School of Marine Science and Technology, Northwestern Polytechnical University, Xi'an 710072, China

[b] Key Laboratory for Unmanned Underwater Vehicle, Northwestern Polytechnical University, Xi'an 710072, China

[c] Unmanned Vehicle Innovation Center, Ningbo Institute of NPU, Ningbo 315105, China

[d] College of Food Science and Engineering, Northwest A&F University, Yangling 712100, Shaanxi, China

*Corresponding authors

E-mail: wanglong79@nwsuaf.edu.cn (J. Wang); zhuwx@nwsuaf.edu.cn (W. Zhu)

Materials and reagents

$Co(NO_3)_2 \cdot 6H_2O$, $Fe(NO_3)_3 \cdot 9H_2O$, ammonium fluoride (NH_4F), urea, $RuCl_3 \cdot 3H_2O$ and $NaH_2PO_2 \cdot H_2O$ were purchased from Aladdin Industrial Corporation (China). Pt/C powder (10%) was purchased from Sigma-Aldrich. Carbon cloth (CC, WOS 1002) was purchased from CeTech Co. Ltd. The water used in all experiments was purified through a Millipore system. All chemicals are in the analytical-reagent grade and were used directly without further purification. The bipolar membrane (BPM, fumasep BIFM) was purchased from Beijing Epsilon Technology Co., Ltd. (China).

Preparation of CoCH NW/CC

A piece of acid-pretreated CC (2 × 3 cm^2) was cleaned with purified water and ethanol for several times. For the synthesis of cobalt carbonate hydroxide (CoCH) nanowires array on CC (CoCH NW/CC), 2 mmol $Co(NO_3)_2 \cdot 6H_2O$, 5 mmol NH_4F and 10 mmol urea were dissolved in 40 mL DI water. After stirring for 10 min, the precursor solution together with the cleaned CC were transferred to a Teflon-lined stainless steel autoclave (50 mL) and heated in an electric oven at 120 °C for 6 h. After that, the CoCH NW/CC was washed with water several times and dried at room temperature. The loading mass of CoCH NW on CC was calculated to be 2.47 mg cm^{-2}.

Preparation of Fe-CoCH NT/CC

The CoCH NW/CC (1 × 1.5 cm^2) was soaked in the $Fe(NO_3)_3 \cdot 9H_2O$ solution with concentrations of 0.1, 0.5, 1, 2, 5, 10 and 20 mM for a certain period of time (0.5, 1, 2, 3 and 5 h) at room temperature. After that, the $Fe(OH)_3$/CoCH nanotubes array on CC (Fe-CoCH NT/CC) was taken out and washed with water several times. Optimum condition is 10 mM and 2 h. The loading mass of Fe-CoCH NT on CC was calculated to be 1.83 mg cm^{-2}.

Preparation of Fe-CoP NT/CC

The Fe-CoCH NT/CC and $NaH_2PO_2 \cdot H_2O$ (200 mg) were placed in two neighbored porcelain boats at the middle of heating zone of the tube furnace. Then, the Fe-CoCH NT/CC was heated for 2 h at 300 °C with a rate of 2 °C min^{-1} under stable argon flow. After that, the iron-cobalt phosphide nanotubes array on CC (Fe-CoP NT/CC) was obtained.

Characterizations

The X-ray diffraction (XRD, Bruker D8 advanced diffractometer) was used to study the phase composition of samples. The scanning electron microscopy (SEM, Hitachi S-4800 field emission scanning electron microscope), energy-dispersive X-ray spectrometry (EDX) and EDX elemental mapping analyses were conducted to study the microstructure, elemental composition and distribution of samples. The transmission electron microscopy (TEM, Hitachi H-8100 electron microscope), high-resolution TEM (HRTEM), selected-area electron diffraction (SAED), scanning TEM (STEM) and STEM-EDX elemental mapping analyses were conducted to study the internal structure, lattice spacing, crystal structure, fine elemental composition and distribution of the Fe-CoCH NT. The X-ray photoelectron spectroscopy (XPS, Thermo Fisher Scientific-Escalab 250Xi) analysis was conducted to study the surface element composition and chemical valence states of samples. Fe leaching in the electrolyte from the Fe-CoCH NT/CC during long-term OER test was analyzed by the ICP-OES (Agilent 5110).

Electrochemical tests

The electrochemical tests of catalysts toward hydrogen evolution reaction (HER), oxygen evolution reaction (OER) and overall water electrolysis were conducted on an electrochemical workstation (CHI 660E, CH Instruments, Inc.). The above-mentioned catalysts (0.25 cm^2) were served as the working electrode. The commercial Hg/HgO (MOE) and Hg/Hg_2Cl_2 (SCE) electrodes were served as the reference electrodes in KOH and H_2SO_4, respectively. A graphite rod was served as the counter electrode. All the linear sweep voltammetry (LSV) curves were recorded at a scan rate of 2 mV s^{-1}. Chronopotentiometry (CP) curves were recorded to study the stability of catalysts toward HER, OER and overall water electrolysis. The potentials of LSV curves against MOE and SCE reference electrodes were converted to reversible hydrogen electrode (RHE) by means of a standard electrochemical method (RHE calibration performed on these two electrodes) proposed by a reported work.[1] The RHE calibrated potentials of MOE and SCE electrodes were tested to be 0.931 and 0.264 V in 1.0 M KOH and 0.5 M H_2SO_4 (temperature of ~24-26 ^oC), respectively. Thus, the conversion formulas are

shown below: E(RHE) = E(MOE) + 0.931 V; E(RHE) = E(SCE) + 0.264 V. The LSV curves are shown with *iR* correction (90%) unless otherwise specified. The LSV curves for overall water electrolysis were collected in the reverse scan direction to avoid the interference of capacitive currents and shown without *iR* correction. The double-layer capacitance (C_{dl}) was evaluated by recording cyclic voltammetry (CV) curves at different scan rates in a non-Faradaic potential window. The electrochemical impedance spectroscopy (EIS) test was conducted under a fixed bias potential with a frequency range of 100 kHz to 0.0005 Hz. In the acid-base hybrid electrolysis (ABE) system, a piece of BPM was used to separate the catholyte (0.5 M H_2SO_4) and anolyte (1.0 M KOH). The Faradaic efficiency of Fe-CoCH NT/CC for alkaline OER was tested by the drainage method. Quantitative comparisons of cell voltages at 10 mA cm^{-2} and quantities of electricity to generate 1.0 Kg H_2 between the alkaline water electrolysis (AWE) and ABE systems were calculated according to previous works.[2,3]

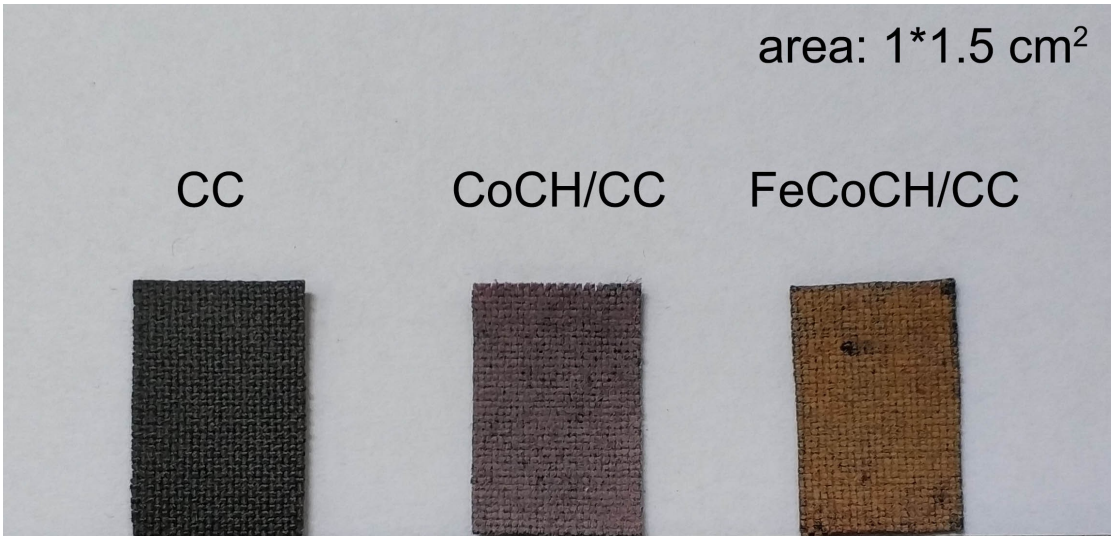

Fig. S1. Optical images of CC, CoCH NW/CC and Fe-CoCH NT/CC.

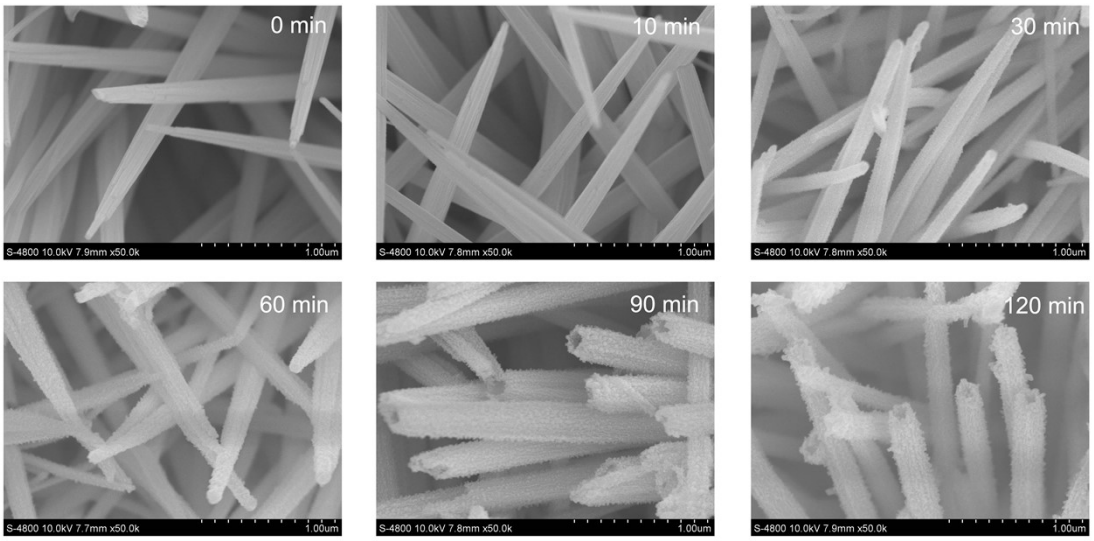

Fig. S2. SEM images of Fe-CoCH/CC synthesized with different Fe^{3+}-soaking time (10 mM).

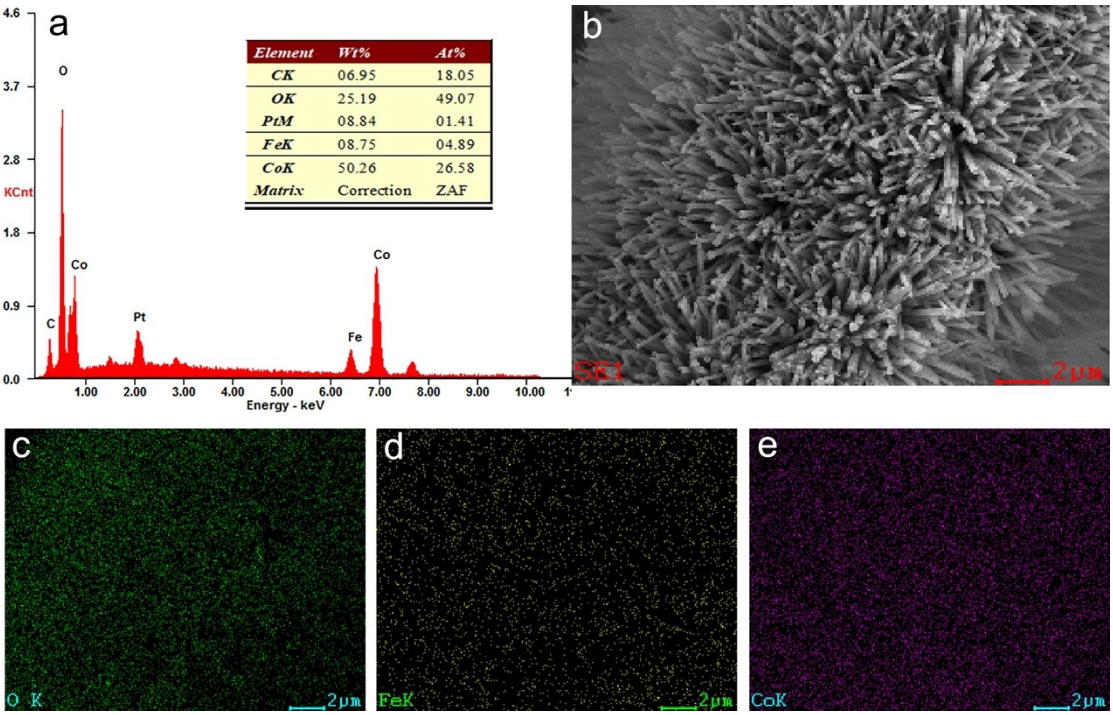

Fig. S3. (a) EDX spectrum and (b-e) EDX elemental mapping of Fe-CoCH NT/CC.

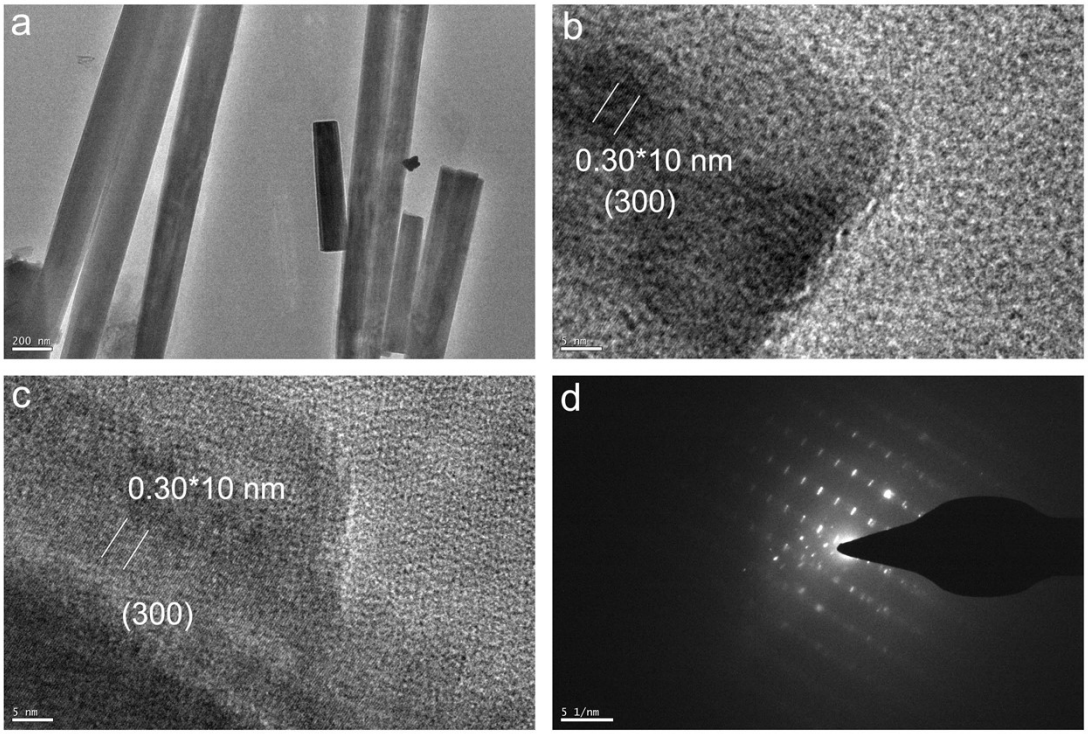

Fig. S4. (a) TEM, (b,c) HRTEM and (d) SAED images of CoCH NW.

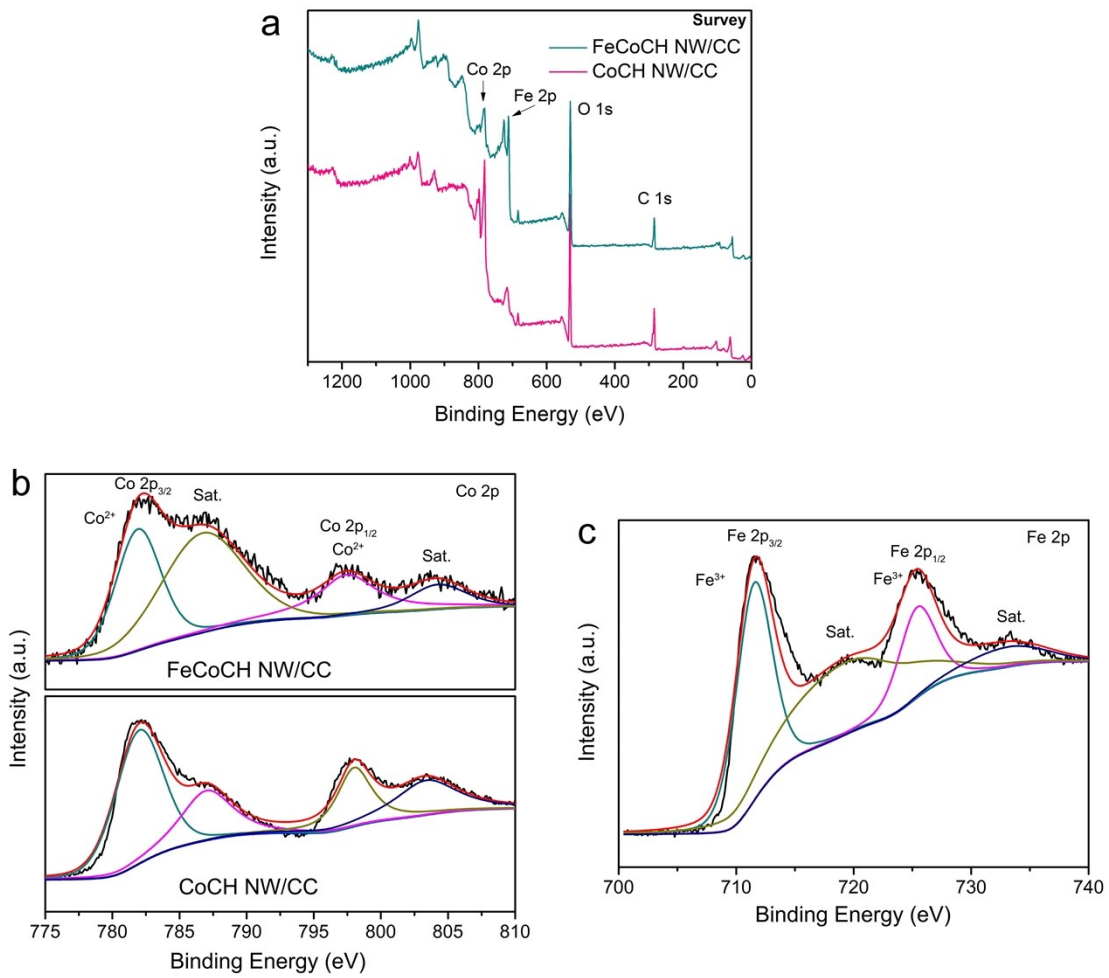

Fig. S5. (a) XPS survey spectra and high-resolution XPS spectra in the regions of (b) Co 2p and (c) Fe 2p of Fe-CoCH NT and CoCH NW.

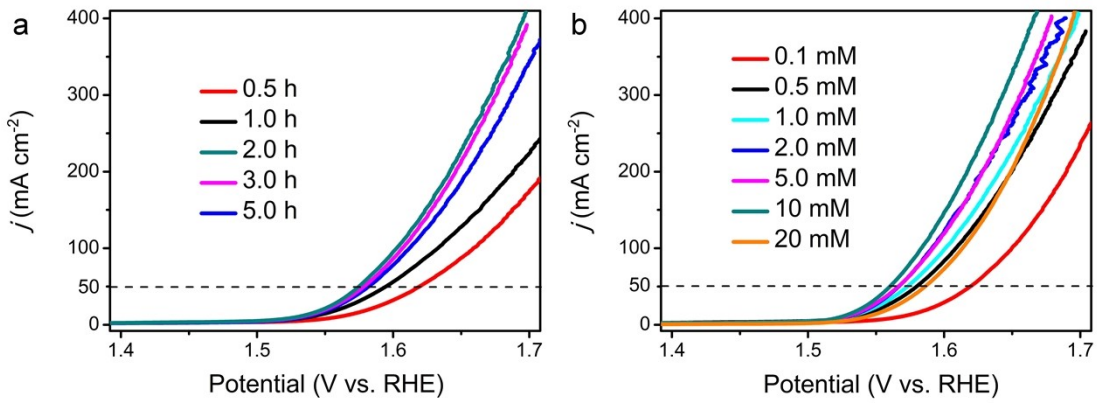

Fig. S6. (a) LSV curves of Fe-CoCH/CC synthesized with different Fe^{3+}-soaking time toward OER in 1.0 M KOH. (b) LSV curves of Fe-CoCH/CC synthesized with different Fe^{3+} concentration toward OER in 1.0 M KOH.

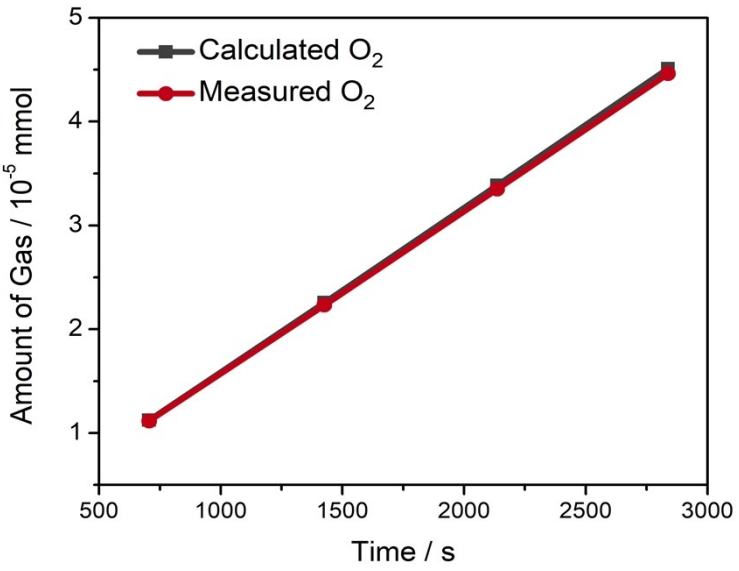

Fig. S7. Faradaic efficiency of Fe-CoCH NT/CC toward OER in 1.0 M KOH.

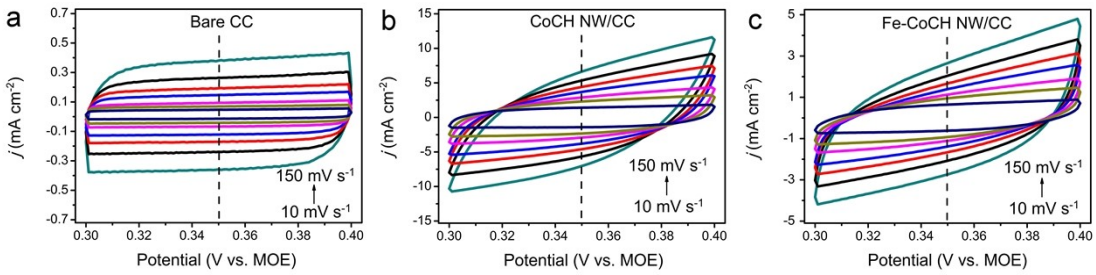

Fig. S8. CV curves recorded at different scan rates of (a) CC, (b) CoCH NW/CC and (c) Fe-CoCH NT/CC in a non-Faradiac potential region in 1.0 M KOH.

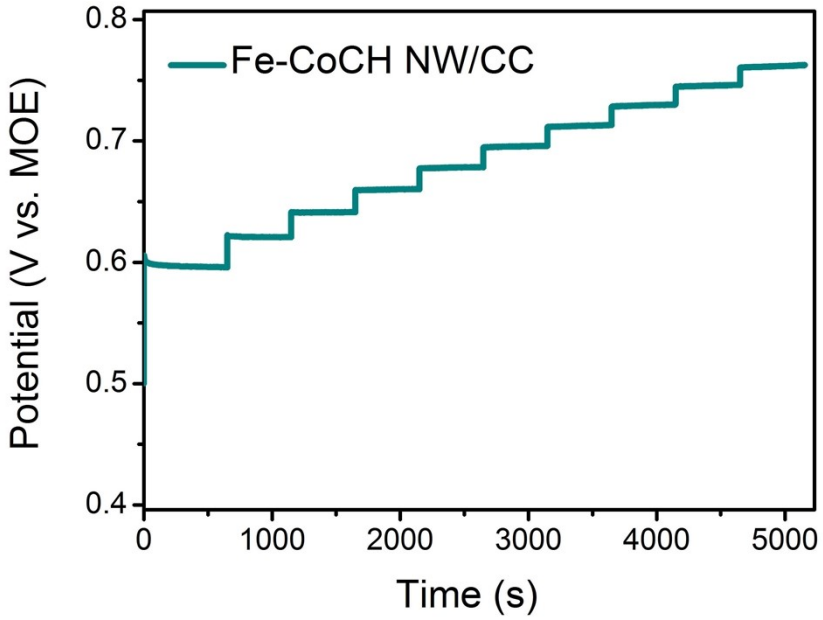

Fig. S9. Multi-step CP curve of Fe-CoCH NT/CC toward alkaline OER with current densities increasing from 10 to 100 mA cm^{-2}.

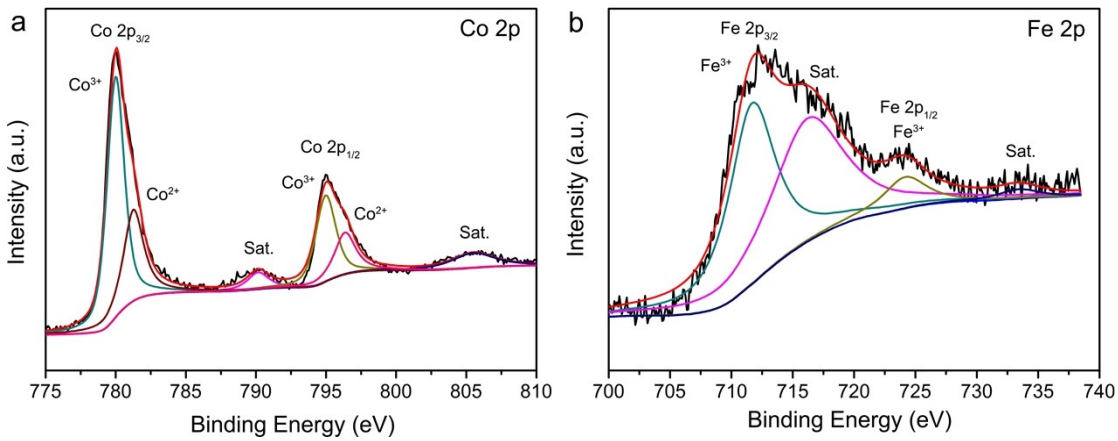

Fig. S10. Deconvoluted high-resolution XPS spectra in the regions of (a) Co 2p and (b) Fe 2p for Fe-CoCH NT/CC after OER CP test.

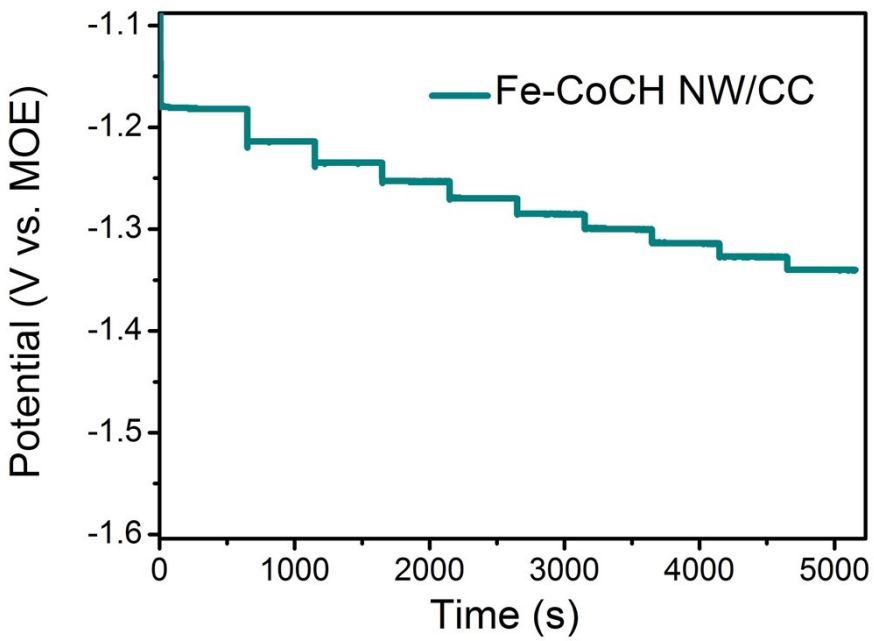

Fig. S11. Multi-step CP curve of Fe-CoCH NT/CC toward alkaline HER with current densities increasing from 10 to 100 mA cm^{-2}.

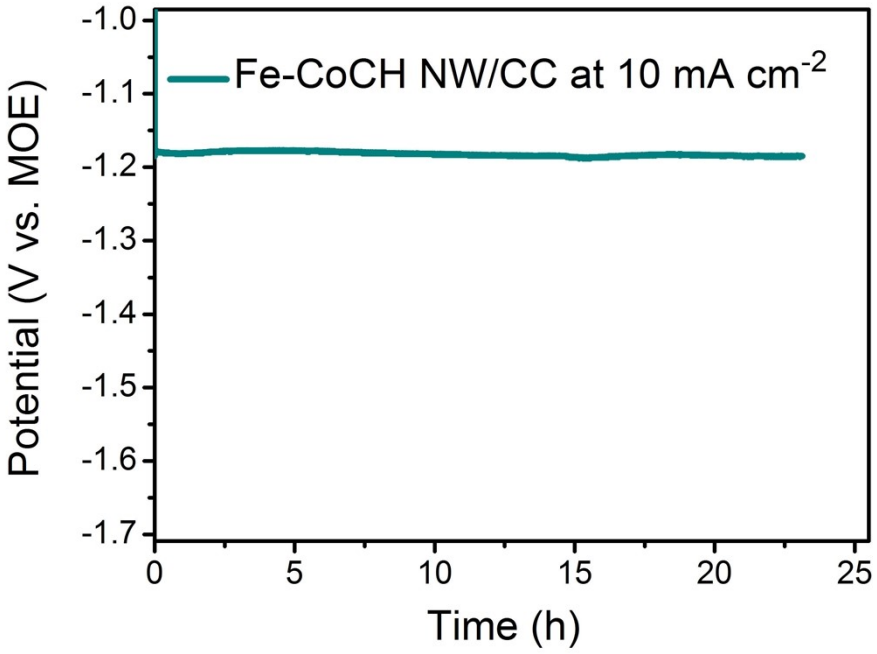

Fig. S12. Long-term CP curve of Fe-CoCH/CC toward alkaline HER at 10 mA cm^{-2}.

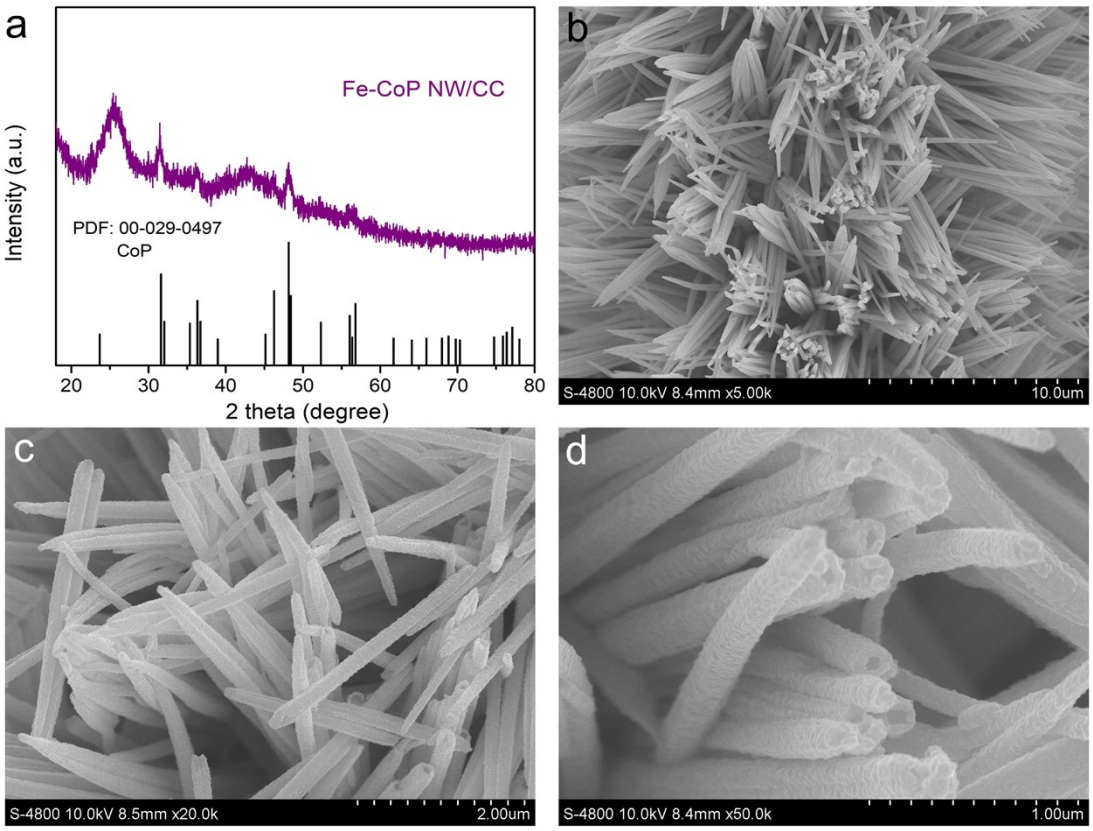

Fig. S13. (a) XRD pattern and (b-d) SEM images of Fe-CoP NT/CC.

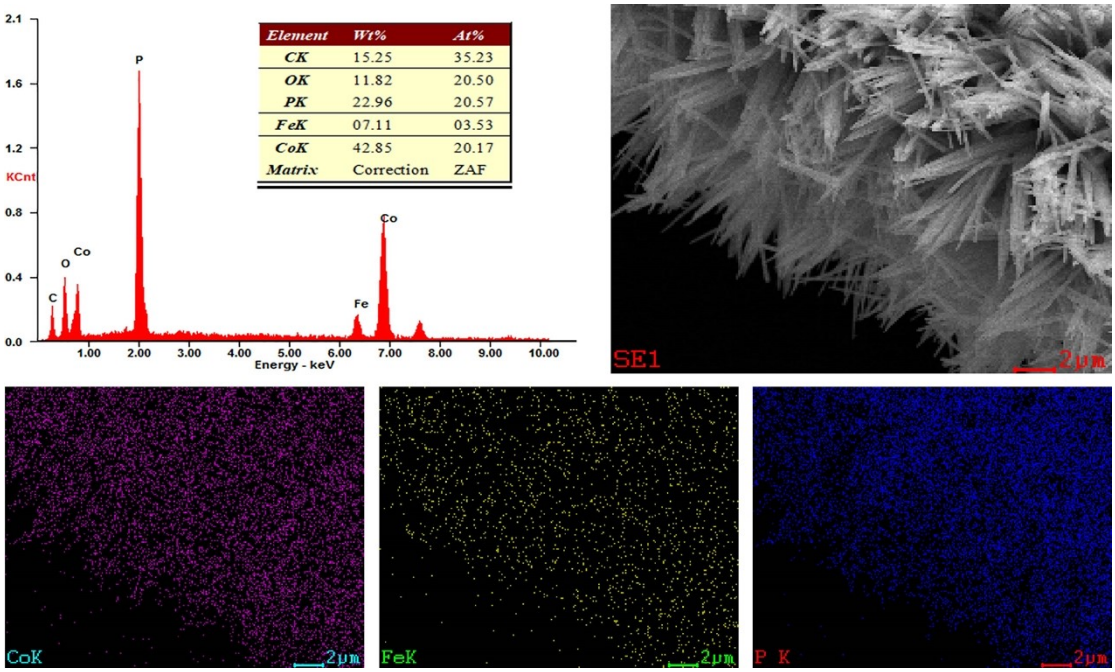

Fig. S14. EDX spectrum and EDX elemental mapping of Fe-CoP NT/CC.

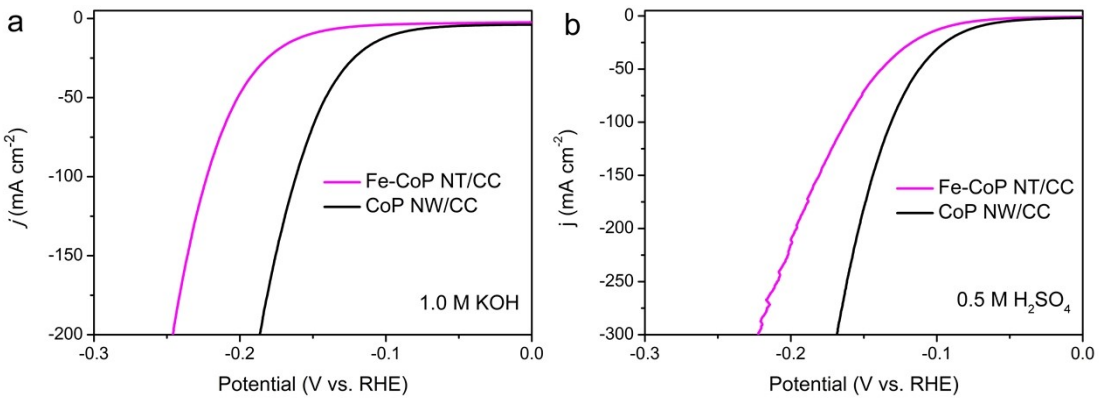

Fig. S15. Comparison of HER performances of Fe-CoCH NT/CC and CoP NW/CC in (a) 1.0 M KOH and (b) 0.5 M H_2SO_4.

Table S1. Performance comparison of alkaline water splitting and acid-base hybrid water splitting systems.

alkaline water splitting system	voltage at 10 mA cm^{-2}	Ref.
Fe-CoCH(+)//Fe-CoP(-)	**1.67**	**this work**
$CoCO_3$@NiFe LDH (-,+)	1.67	4
Mo-Ni_3S_2 (-,+)	1.67	5
Mn-CoP/Co_2P (-,+)	1.67	6
Cu_2Se@NiFe-LDH (-,+)	1.67	7
Co_1Mn_1CH/NF (-,+)	1.68	8
CoP@FeCoP (-,+)	1.68	9
Ce-NiCo-LDH/NF (-,+)	1.68	10
NiFeB@OCC (-,+)	1.69	11
0.1Fe-NiS/MoS_2 (-,+)	1.66	12

Table S2. Performance comparison of alkaline water splitting and acid-base hybrid water splitting systems.

acid-base water splitting system	**voltage at 1/10 mA cm^{-2}**	**Ref.**
Fe-CoCH(+)//Fe-CoP(-)	**0.97 at 10 mA cm^{-2}**	**this work**
CoP NS/CC (-,+)	0.735 V at 1 mA cm^{-2} 0.9 V at 10 mA cm^{-2}	13
Pt/C(-)//$MnCo_2O_4$@NiFeRu-LDH (+)	0.59 V at 10 mA cm^{-2}	14
Ni_2P (-,+)	0.79 V at 1 mA cm^{-2} ~1.13 V at 10 mA cm^{-2}	15
Ru-RuO_2/CNT (-,+)	0.73 V at 10 mA cm^{-2}	16
V_8C_7/CoP (-,+)	0.8 V at 10 mA cm^{-2}	17

Reference

[1] S. Niu, S. Li, Y. Du, X. Han and P. Xu, How to reliably report the overpotential of an electrocatalyst, *ACS Energy Lett.*, 2020, **5**, 1083-1087.

[2] W. Zhu, X. Fu, A. Wang, M. Ren, Z. Wei, C. Tang, X. Sun and J. Wang, Energy-efficient electrolytic H_2 production and high-value added H_2-acid-base co-electrosynthesis modes enabled by a Ni_2P catalyst in a diaphragm cell, *Appl. Catal. B-Environ.*, 2022, **317**, 121726.

[3] C. Lu, S. Yang, Y. Zhao, Y. Cao, Q. Huang, W. Zhu and J. Wang, Energy-saving and sustainable saline-base electrolytic hydrogen production system enabled by nickel sulfide-based catalysts, *J. Mater. Chem. A*, 2023, **11**, 22216-22222.

[4] R. Que, S. Liu, P. He, Y. Yang and Y. Pan, Hierarchical heterostructure $CoCO_3$@NiFe LDH nanowires array as outstanding bifunctional electrocatalysts for overall water splitting, *Mater. Lett.*, 2020, **277**, 128285.

[5] C. Wu, B. Liu, J. Wang, Y. Su, H. Yan, C. Ng, C. Li and J. Wei, 3D structured Mo-doped Ni_3S_2 nanosheets as efficient dual-electrocatalyst for overall water splitting, *Appl. Surf. Sci.*, 2018, **441**, 1024-1033.

[6] F. Tang, Y. Zhao, Y. Ge, Y. Sun, Y. Zhang, X. Yang, A. Cao, J. Qiu and X. Lin, Synergistic effect of Mn doping and hollow structure boosting Mn-CoP/Co_2P nanotubes as efficient bifunctional electrocatalyst for overall water splitting, *J. Colloid Interf. Sci.*, 2022, **628**, 524-533.

[7] H. Qi, P. Zhang, H. Wang, Y. Cui, X. Liu, X. She, Y. Wen and T. Zhan, Cu_2Se nanowires shelled with NiFe layered double hydroxide nanosheets for overall water-splitting, *J. Colloid Interf. Sci.*, 2021, **599**, 370-380.

[8] T. Tang, W. Jiang, S. Niu, N. Liu, H. Luo, Y. Chen, S. Jin, F. Gao, L. Wan and J. Hu, Electronic and morphological dual modulation of cobalt carbonate hydroxides by Mn doping toward highly efficient and stable bifunctional electrocatalysts for overall water splitting, *J. Am. Chem. Soc.*, 2017, **139**, 8320-8328.

[9] J. Shi, F. Qiu, W. Yuan, M. Guo and Z. Lu, Nitrogen-doped carbon-decorated yolk-shell CoP@FeCoP micro-polyhedra derived from MOF for efficient overall water splitting, *Chem. Eng. J.*, 2021, **403**, 126312.

[10] H. N. Dhandapani, D. Mahendiran, A. Karmakar, P. Devi, S. Nagappan, R. Madhu, K. Bera, P. Murugan, B. R. Babu and S. Kundu, Boosting of overall water splitting activity by regulating the electron distribution over the active sites of Ce doped NiCo-LDH and atomic level understanding of the catalyst by DFT study, *J. Mater. Chem. A*, 2022, **10**, 17488-17500.

[11] A. Kafle, D. Gupta and T. C. Nagaiah, Facile fabrication of NiFeB deposited flexible carbon cloth electrode towards overall water splitting in alkaline and saline solutions, *Electrochim. Acta*, 2023, **441**, 141779.

[12] P. Liu, J. Li, J. Yan and W. Song, Defect-rich Fe-doped NiS/MoS_2 heterostructured ultrathin nanosheets for efficient overall water splitting, *Phys. Chem. Chem. Phys.*, 2022, **24**, 8344-8350.

[13] W. Zhu, W. Zhang, Y. Li, Z. Yue, M. Ren, Y. Zhang, N. M. Saleh and J. Wang, Energy-efficient 1.67 V single- and 0.90 V dual-electrolyte based overall water-electrolysis devices enabled by a ZIF-L derived acid-base bifunctional cobalt phosphide nanoarray, *J. Mater. Chem. A*, 2018, **6**, 24277-24284.

[14] Z. Wang, P. Cai, Q. Chen, X. Yin, K. Chen, Z. Lu and Z. Wen, Development of high-efficiency alkaline OER electrodes for hybrid acid-alkali electrolytic H_2 generation, *J. Colloid Interf. Sci.*, 2023, **636**, 610-617.

[15] Y. Li, J. Chen, P. Cai and Z. Wen, An electrochemically neutralized energy-assisted low-cost acid-alkaline electrolyzer for energy-saving electrolysis hydrogen generation, *J. Mater. Chem. A*, 2018, **6**, 4948-4954.

[16] M. Zhang, J. Chen, H. Li, P. Cai, Y. Li and Z. Wen, Ru-RuO_2/CNT hybrids as high-activity pH-universal electrocatalysts for water splitting within 0.73 V in an asymmetric-electrolyte electrolyzer, *Nano Energy*, 2019, **61**, 576-583.

[17] L. Wu, M. Zhang, Z. Wen and S. Ci, V_8C_7 decorating CoP nanosheets-assembled microspheres as trifunctional catalysts toward energy-saving electrolytic hydrogen production, *Chem. Eng. J.*, 2020, **399**, 125728.